Influence of Fouling on Compressor Dynamics: Experimental and Modelling Approach

Jombo, Gbanaibolou[1]
Centre for Propulsion Engineering, School of Aerospace, Transport & Manufacturing, Cranfield University, UK
g.jombo@cranfield.ac.uk

Pecinka, Jiri
Department of Air Force and Aircraft Technology, University of Defence, Czech Republic
jiri.pecinka@unob.cz

Sampath, Suresh
Centre for Propulsion Engineering, School of Aerospace, Transport & Manufacturing, Cranfield University, UK

Mba, David
Faculty of Technology, De Montfort University, Leicester, UK

ABSTRACT

The effect of compressor fouling on the performance of a gas turbine has been the subject of several papers; however, the goal of this paper is to address a more fundamental question of the effect of fouling, which is the onset of unstable operation of the compressor. Compressor fouling experiments have been carried out on a test rig refitted with TJ100 small jet engine with centrifugal compressor. Fouling on the compressor blade was simulated with texturized paint with average roughness value of 6 microns. Compressor characteristic was measured for both the clean (baseline) and fouled compressor blades at several rotational speeds by throttling the engine with variable exhaust nozzle. A Greitzer-type compression system model has been applied based on the geometric and performance parameters of the TJ100 small jet engine test rig. Frequency of plenum pressure fluctuation, the mean disturbance flow coefficient and pressure-rise coefficient at the onset of plenum flowfield disturbance predicted by the

[1] Jombo, Gbanaibolou, Cranfield University, UK; Email: g.jombo@cranfield.ac.uk

model was compared with the measurement for both the baseline and fouled engine. Model prediction of the flowfield parameters at inception of unstable operation in the compressor showed good agreement with the experimental data. The results proved that used simple Greitzer model is suitable for prediction of the engine compressor unstable behaviour and prediction of the mild surge inception point for both the clean and the fouled compressor.

Keywords: *Compressor Fouling, Compressor Modelling, Greitzer Model, Compressor Flowfield Disturbance, TJ100*

1.0 INTRODUCTION

Compressor fouling is the deposition of airborne contaminates such as fly ash, airborne salt, hydrocarbon, dust, lube oil, etc. on the surfaces of the compressor blades, stators and annulus walls [1–3]. It is estimated to account for 70-85% of the performance losses in a gas turbine, making fouling in compressors a serious problem for gas the turbine operator [4].

The rate of fouling in a compressor is affected by the type of the environment (e.g. desert, offshore, tropic or artic), the type of location (e.g. industrial, urban or countryside), the atmospheric condition (e.g. rain, humidity or fog) and the position & elevation of the intake [2,3]. The principal effect of fouling on a compressor's performance is manifested by a drop in the compressor's air mass flow, efficiency, pressure ratio and power output [5].

The detrimental effect of compressor fouling on the overall performance of a gas turbine can be controlled through effective inlet air filtration systems combined with a suitable mix of online and offline compressor washing.

Previous works on the effect of fouling on gas turbine compressor dynamics has been on estimating its effect on engine performance in terms of reduction in power output and thermal efficiency. Aker and Saravanamuttoo [6] have applied a stage stacking compressor model and a linear fouling assumption to investigate the performance deterioration of fouling in the compressor. Rodriguez et al. [7] has further improved on the work by Aker and Saravanamuttoo [6] by including the effect of stage temperature rise coefficient deterioration to the Aker model. Melino et al. [8] have also adopted the stage stacking compressor model to investigate the performance deterioration effect of compressor fouling. Yang and Xu [9] has modelled the effect of fouling on the performance of a multi-stage compressor.

Another approach used by several investigators to determine the effect of fouling on a gas turbine compressor dynamics involved the formulation of correlations to characterizing the sensitivity and susceptibility of the compressor to fouling. Tarabin et al. [10] proposed a susceptibility index to access the performance deterioration of a compressor due to fouling based on the principle for the entrainment efficiency of a cylinder due to inertia deposition. Song et al. [11] has improved on the work by Tarabin [8] to account better for the flow around a real blade. Seddigh and Saravanamuttoo [12] have proposed a fouling index to quantify the susceptibility of a compressor to fouling. Kurz and Brun [3] have looked at the fouling mechanism leading to the deposition of particles on either the suction or pressure side of the compressor aerofoil. Based on experimental data, they have identified the size of the particle, wetness of the particle

or aerofoil surface and the quality of inlet air filtration as the dominant fouling susceptibility factors [3].

In this paper, the fundamental question addressed is modelling the effect of fouling on the inception of unstable operations in a fouled compressor. This is important as fouling has been noted to cause surge in compressors mainly due to a reduction in the compressors surge margin [13].

A Greitzer-type compression system model was applied to predict the unstable operations parameters of a fouled compressor. Greitzer [14] presented a nonlinear lumped parameter model for axial compressors capable of describing oscillations during a surge cycle. This type of model is the most widely used dynamic model in the field. Later on Hansen et al. [15] proved that the model is also suitable for centrifugal compressor systems. The model was continuously developed by Moore and Greitzer [16] who presents a model capable of describing not just surge but also a rotating stall and possible coupling between the two instabilities. Fink et al. [17] added rotor dynamics to the Greitzer model to account for the effect of speed variations. Similar model was developed by Gravdahl and Egeland [18], and further expanded to include the equations for rotating stall [19]. Macdougal and Elder [20] addressed expanding the Greitzer model by adding the compressibility effect. A sophisticated two-dimensional, compressible flow model for centrifugal and axial compressors was developed by Spakovszky [21].

Only the simplest form of the Greitzer model considering just one-dimensional flow (surge) is used in presented paper. A small jet test rig, on which the compressor

fouling experiment was performed forms the basis for the validation of a Greitzer-type compression system model and its potential to reflect changes in compressor behaviour caused by fouling.

2.0 TESTING AND MEASUREMENTS

Compressor fouling experiment was conducted utilizing a small jet engine designated TJ100. The engine has centrifugal compressor with radial and axial bladed diffusers, reversed flow combustor and single stage axial turbine. The compressor design pressure ratio is approximately 4.5, rated maximum rotational speed of approximately 60,000 RPM and the engine maximum thrust is 1kN [22]. A variable exhaust nozzle can be optionally fitted to the engine. Engine compressor inlet and discharge total pressures and temperatures were measured and evaluated together with the engine air mass flow rate. Engine layout together with all measurement parameters and their respective positions are depicted in Fig. 1.

Engine gas path temperatures (i.e. T_i) and engine performance parameters measurements (i.e. rotational speed) were performed at 50 Hz sampling rate while gas path pressures (i.e. P_i) were measured at 1 kHz rate.

At first, engine parameters with clean compressor engine configuration were measured as a baseline. Engine steady state operating line was measured in the range from idle (50%) to 95% of max. design rotational speed with fixed exhausted nozzle. Subsequently constant speed lines were evaluated by throttling the engine (compressor) mass flow with a variable exhaust nozzle while the engine control system was maintaining constant engine rotating speed. At each speed line the engine was

throttled until unstable compressor operation, which was estimated based on the air mass flow rate oscillations displayed to the test operator and based on the engine audible noise. The resolution between two adjacent points on a speed lines is approximately 2% of the engine rated air flow rate. Steady state parameters were calculated as average from 1 second long data waveform.

Consequently the compressor was fouled with a paint applied to the inducer suction side surface based on the real fouling pattern observed at the particular engine (Fig. 2). In order to increase roughness of the treated surface the paint was structured with micro glass balls sizing from 1 to 50μm. The balls were mixed with the paint in 1:1 mass ratio. The resulting paint layer thickness was approximately 65μm and roughness Ra=6μm (Fig. 3). The original roughness of a clean blade was Ra=0.8μm.

The compressor pressure map measurement was then repeated for the fouled condition. Comparison of both the clean and the fouled compressor pressure map is depicted in Fig. 4.

Furthermore, Fig. 4 shows the compressor operating line for both the clean and fouled compressor and also the surge or instability inception points. Evident from Fig 4 and also reported by other investigators [4,5], fouling causes a displacement of the compressor operating line to the left and also reduces the surge margin, as such, the fouled compressor surges earlier than the clean compressor.

The compressor map is generalized using Equations (5) and (6) and used for the creation of the compression system model. The non-dimensional form of the

compressor map for speed lines form 80% to 95% with highlighted unstable operating points is presented in Fig. 5.

The compressor discharge pressure oscillations at the unstable operating points were analyzed in both time and frequency domain. The pressure oscillations with frequency around 55 Hz were observable in all the pressure signals and engine speeds. The oscillation frequency well correlates with the calculated system Helmholtz frequency ω_H = 59 Hz calculated from Equation (1). This suggests that the detected instability was a mild surge. More detailed analysis of the engine behaviour at mild surge is described in [23]

$$\omega_H = a\sqrt{\frac{A_c}{V_p L_c}} \tag{1}$$

where ω_H is the Helmholtz frequency, a is the speed of sound at the sea level static conditions, V_p is the plenum volume, A_c is the compressor annulus flow area, L_c is the effective length of the compressor and the ducting.

An example of time waveform and frequency spectrum for the mild surge point and two other at higher flow rate for 90% engine rotational speed is depicted in Fig. 6. Mean (time averaged) flow coefficient, mean pressure-rise coefficient and frequency of plenum pressure oscillations at the mild surge points were subsequently compared with the model for both the clean and fouled compressor configuration.

3.0 TESTING AND MEASUREMENTS

3.1 Greitzer Compression System Model

The Greitzer [14] compression system model as shown in Fig. 7 is a lumped parameter model consisting of a compressor operating in a duct and discharging to plenum with a throttle to control the flow through the compression system. It's suitable for modelling the surge dynamics in a compressor.

The governing equation for the Greitzer compression system are [14,15]:

$$\frac{d\Phi_c}{dt} = B\left(\Psi_c - \Psi_p\right) \tag{2}$$

$$\frac{d\Phi_{th}}{dt} = \left(\frac{B}{G}\right)\left(\Psi_p - \Psi_{th}\right) \tag{3}$$

$$\frac{d\Psi_p}{dt} = \left(\frac{1}{B}\right)\left(\Phi_c - \Phi_{th}\right) \tag{4}$$

$$\frac{d\Psi_c}{dt} = \left(\frac{1}{\tau}\right)\left(\Psi_{c,ss} - \Psi_c\right) \tag{5}$$

where Φ_c & Φ_{th} are the flow coefficients in the compressor & throttle respectively, Ψ_p & Ψ_c are pressure-rise coefficient for the plenum and compressor respectively, $\Psi_{c,ss}$ is the steady state compressor pressure-rise characteristics, B is the Greitzer parameter, G is a geometric parameter and τ is the compressor flow relaxation time.

The non-dimensional compressor flow coefficient (Φ_c) is expressed as [14]:

$$\Phi_c = \frac{C_x}{U} = \frac{\rho C_x A_c}{\rho U A_c} = \frac{\dot{m}}{\rho U A_c} \tag{6}$$

where C_x is the axial velocity, U is the impeller tip speed, ρ is the average density of the air in the compressor, A_c is the compressor inlet annulus area and $\dot{m}$ is the mass flow rate.

The non-dimensional compressor pressure-rise coefficient (Ψ_c) is expressed as [14]:

$$\Psi_c = \frac{\Delta P}{\frac{1}{2}\rho U^2} = \frac{P_1(PR-1)}{\frac{1}{2}\rho U^2} \tag{7}$$

where ΔP is the pressure rise from the compressor inlet to the plenum, P_1 is the compressor inlet pressure and PR is the compressor pressure ratio.

The throttle pressure-rise coefficient (Ψ_{th}) is expressed as [15]:

$$\Psi_{th} = S\Phi_{th}^2 \tag{8}$$

where S is the throttle parameter and Φ_{th} is the throttle flow coefficient.

The throttle parameter (S) based on the work by Hansen et al. [15], is expressed as:

$$S = \left(\frac{A_c}{A_v}\right)^2 \tag{9}$$

where A_c is the compressor inlet flow area and A_v is the throttle valve throat area at a point in time.

The throttle parameter represents the geometric characteristic of the throttle valve and its percentage opening at a particular point in time.

A preferable representation of the throttle parameter based on the work by Yoon et al. [24], is:

$$S = (c_{th}u_{th})^2 \tag{10}$$

where c_{th} is the throttle valve constant for the specific valve geometry and u_{th} is the percentage opening of the throttle valve.

The Greitzer parameter (B) is expressed as [14]:

$$B = \frac{U}{2a}\sqrt{\frac{V_p}{A_c L_c}} \tag{11}$$

where U is the tip speed of the impeller, a is the speed of sound at the ambient condition, V_p is the plenum volume, A_c is the compressor inlet flow area, L_c is the effective length of the compressor and the ducting.

The geometric parameter (G) is expressed as [14]:

$$G = \frac{\left(\frac{L_T}{A_T}\right)}{\left(\frac{L_c}{A_c}\right)} \tag{12}$$

where L_T & L_C are the effective length of the throttle and compressor respectively and A_T & A_c are the flow areas of the throttle and compressor respectively.

The compressor flow relaxation time (τ) is expressed as [14]:

$$\tau = \frac{\pi R N}{L_c B} \tag{13}$$

where $R$is the compressor mean radius, N is the time lag in revolution, L_c is the effective length of the compressor and B is the Greitzer B parameter.

The time lag parameter N was chosen based on the recommendation of Hansen et al. [15], where N=0.5 for centrifugal compressors. Although in the original Greitzer [14] axial compression system model, the time lag parameter was 2; Hansen et al. [15] argued based on their experimental data, that for centrifugal compressors, the time lag for transitioning from un-stalled to fully stalled mode was quite shorter as compared to the axial compressor.

4.0 RESULTS & DISCUSSION

Fig. 8 summarizes the geometric parameters for the TJ100 small jet engine test rig necessary for the Greitzer compression system model.

4.1 Generalized Compressor Pressure-rise Characteristic

The generalized steady-state compressor pressure-rise characteristic is a graphical representation of the relationship between the non-dimensional pressure-rise coefficient and the non-dimensional flow coefficient in the compressor when operating in steady state conditions.

The generalized pressure-rise characteristic for the baseline and fouled TJ100 engine is presented in Fig. 9 based on experimental compressor pressure map in Fig. 4.

The polynomial curve fitting is based on the Moore and Greitzer [16] recommendation for the general form of the compressor pressure-rise characteristic.

From Fig. 9, the steady state generalized pressure-rise characteristic for the baseline and fouled TJ100 compressor are:

$$\Psi_{c,ss}^{base} = -145.42\ \Phi_c^3 + 59.72\Phi_c^2 - 0.6074\Phi_c + 1.5 \tag{14}$$

$$\Psi_{c,ss}^{foul} = -145.31\Phi_c^3 + 58.583\Phi_c^2 - 0.4918\Phi_c + 1.55 \tag{15}$$

4.2 Model Validation and Simulation

The governing equations for the Greitzer compression system given in Equations (2) - (5) have been implemented in MATLAB using the ODE45 module to simultaneously solve the 4 sets of first-order differential equations.

The Greitzer model prediction for the following parameters: frequency of plenum pressure disturbance, mean disturbance flow coefficient and pressure-rise coefficient at the inception of unstable operation in the compressor was compared against the

experimental data for the speed lines (80%, 85%, 90% & 95% of rated max. speed). Throttle parameter S corresponding with the inception of instability for all examined speeds and both baseline and fouled conditions are presented in Table 1.

It is possible to see that for the fouled condition the instability appeared for higher throttle parameter S, this means higher flow area. Unfortunately the throttle area was not measured during the experiment, thus the results cannot be compared.

4.3 Results Comparison

Fig. 10 shows the frequency of the plenum pressure disturbance at the inception of unstable operations in the compressor for both the baseline and fouled engine respectively. Comparison of the experimental data (solid lines) and the Greitzer model prediction (dashed line) is presented for different relative speeds.

When operated at 90% of its rated speed the TJ100 compression system, the plenum pressure disturbance has lower frequency than at the rest of the speeds. This was true for both the baseline and the fouled condition, as seen in Fig. 10; the Greitzer model was able to capture this behaviour very well.

In Fig. 11 the mean (time averaged) flow coefficients at the inception of unstable compressor operation for the baseline and fouled compressor are compared at different relative speeds. A moderate rising trend in the stall inception flow coefficient with the compressor speed is apparent for the experimental data. Additionally with the fouled compressor, the mild surge was incepted at significantly higher flow coefficient at 90% of the engine speed; this can be also observed in Fig. 5. On the other hand the model predicts nearly constant flow. The almost flat shape of the model prediction for the

mean flow coefficient stems from the data averaging employed in generating the generalized compressor pressure-rise characteristic. From Fig. 9, it can be seen that the generalized compressor pressure-rise characteristics is a best-fit relationship between the pressure-rise coefficient and flow coefficient for all speed lines of a particular compressor and health state. This makes the point of inception of unstable operation in the compressor for all the speed lines to collapse to a single point. Consequently, the model based on this best fit curve predicts almost constant flow coefficient at the instability inception for the particular health state. However, real instability inception exhibits some drift and scatter. This has also been observed experimentally by Aretakis et al. [25] with a turbocharger centrifugal compressor.

Fig. 12 compares the mean (time averaged) pressure-rise coefficient for both the baseline and fouled compressor at the inception of unstable operation in the compressor at different relative speeds. During the experiment, the instability inception appeared at lower pressure-rise coefficient for the 90% of the relative operating speed for both the clean and fouled state. The model prediction of the mean pressure-rise coefficient follows similar trends as observed in the experiment. This further highlights the flexibility of the Greitzer model in predicting the peculiar dynamic behaviour of the test rig compressor at 90% of its rated speed.

The measured and simulated time waveforms of the plenum pressure-rise coefficient for the baseline (clean) engine at 85% rated speed are presented in Fig. 13. Although the Greitzer model predicts quite accurately the frequency of plenum pressure-rise disturbance and its mean value, it does not capture the variance in the amplitude of the

pressure-rise disturbance observed in the experimental data in Fig. 13. The level of the real compressor operation instability is significantly changing, with the lowest pressure-rise amplitudes correlating well with the ones predicted by the model. The Greitzer model based on the generalized compressor pressure-rise characteristic is predicting oscillations with constant amplitude as long as the throttling parameter is kept constant. In General, the order of magnitude of Greitzer model prediction of the amplitude of plenum pressure-rise coefficient show good agreement with the measured experimental result.

5.0 CONCLUSION

A lumped parameter model based on the Greitzer [14] compression system model as modified by Hansen et al. [15] for the centrifugal compressor has been built to verify its capability to simulate the dynamic behaviour of a clean and fouled centrifugal compressor when operating in unstable conditions.

The prediction of the plenum pressure disturbance frequency, mean flow coefficient and mean pressure-rise coefficient at the inception of unstable operations in the compressor by the Greitzer compression model was compared with the experimental data at different operation speeds. The results show very good agreement especially for the plenum pressure frequency. Calculated pressure-rise coefficient also correlates with the experiment well. The flow coefficient shows good correlation in average value; however, the model did not capture a moderate rising trend with the compressor speed present in the experimental data. The model also failed in detection of significantly higher flow coefficient at mild surge inception for the 90% speed of the

fouled compressor. Although the model's prediction of the order of magnitude of the plenum pressure-rise coefficient showed good agreement with the experimental data, it failed to capture, the observed variance in the amplitude of the plenum disturbance observed in the experimental data.

However, the results proved that the used simple Greitzer model is suitable for prediction of the engine compressor unstable behaviour and prediction of the mild surge inception point for both the clean and the fouled compressor.

Finally, the model was able to partially capture different engine behaviour for the 90% speed. Better correlation for this particular speed might be achieved provided that the speed averaged generalized compressor pressure-rise characteristic used for the model in whole speed range would be replaced by one more precisely matching to the particular speed line.

ACKNOWLEDGMENT

Research was supported by the manufacturer of the tested small jet engine - PBS Velká Bíteš, a.s

FUNDING

This work was funded by the Ministry of Defence of the Czech Republic under the framework of Project for the Organization Development - LETKONF.

NOMENCLATURE

a	speed of sound at the ambient condition
A_c	compressor inlet annulus flow area
A_T	throttle flow area
A_V	throttle valve throat area
B	Greitzer parameter
c_{th}	Throttle valve constant for the specific valve geometry
C_x	axial velocity
G	geometric parameter
L_c	effective length of the compressor and the ducting
L_T	effective length of the throttle
$\dot{m}$	massflow
N	time lag in revolution
N_{rel}	relative speed
P_1	compressor inlet pressure
PR	pressure ratio
R	compressor mean radius
R_a	roughness value
S	throttle parameter
U	impeller tip speed
u_{th}	Percentage opening of the throttle valve
V_p	plenum volume

Greek Symbols

Φ_c & Φ_{th}	flow coefficient in the compressor & throttle respectively
Ψ_p & Ψ_c	pressure-rise coefficient for the plenum and compressor respectively
Ψ_{th}	throttle pressure-rise coefficient
$\Psi_{c,ss}$	steady state compressor pressure-rise characteristics
τ	compressor flow relaxation time
ρ	average density of air in the compressor
ΔP	pressure rise from the compressor inlet to the plenum
ω_H	Helmholtz frequency

REFERENCES

[1] Igie, U., Pilidis, P., Fouflias, D., Ramsden, K., and Laskaridis, P., 2014, "Industrial Gas Turbine Performance: Compressor Fouling and On-Line Washing," J Turbomach, **136**(10), pp. 101001–13.

[2] Meher-homji, C. B., Focke, A. B., and Wooldridge, M. B., 1989, "Fouling of Axial Flow Compressors - Causes, Effcets, Detention, And Control," *Proceedings of the Eighteenth Turbomachinery Symposium*, Texas A&M University, Texas, USA, pp. 55–76.

[3] Kurz, R., and Brun, K., 2012, "Fouling Mechanisms in Axial Compressors," J Eng Gas Turb Power, **134**(3), pp. 32401–32409.

[4] Meher-Homji, C. B., and Bromley, A., 2004, "Gas Turbine Axial Compressor Fouling and Washing," *Proceedings of the Thirty-Third Turbomachinery Symposium*, pp. 163–191.

[5] Kurz, R., and Brun, K., 2000, "Degradation in Gas Turbine Systems," J Eng Gas Turb Power, **123**(1), pp. 70–77.

[6] Aker, G. F., and Saravanamuttoo, H. I. H., 1989, "Predicting Gas Turbine Performance Degradation Due to Compressor Fouling Using Computer Simulation Techniques," J Eng Gas Turb Power, **111**(2), pp. 343–350.

[7] Rodríguez, C., Sánchez, D., Chacartegui, R., Muñoz, A., and Martínez, G. S., 2013, "Compressor Fouling: A Comparison of Different Fault Distributions Using a 'Stage-Stacking' Technique," *ASME Turbo Expo 2013: Turbine Technical Conference and Exposition Volume 2: Aircraft Engine; Coal, Biomass and Alternative Fuels; Cycle Innovations San Antonio, Texas, USA, June 3–7, 2013*, ASME, San Antonio, Texas.

[8] Melino, F., Peretto, A., and Spina, P. R., 2010, "Development and Validation of a Model for Axial Compressor Fouling Simulation," *ASME Turbo Expo 2010: Power for Land, Sea, and Air Volume 5: Industrial and Cogeneration; Microturbines and Small Turbomachinery; Oil and Gas Applications; Wind Turbine Technology Glasgow, UK, June 14–18, 2010*, ASME, Glasgow, UK, pp. 87–98.

[9] Yang, H., and Xu, H., 2014, "The New Performance Calculation Method of Fouled Axial Flow Compressor," Sci. World J., **2014**, pp. 1–10.

[10] Tarabrin, A. P., Schurovsky, V. A., Bodrov, A. I., and Stalder, J.-P., 1998, "An Analysis of Axial Compressor Fouling and a Blade Cleaning Method," J Turbomach, **120**(2), pp. 256–261.

[11] Song, T. W., Sohn, J. L., Kim, T. S., Kim, J. H., and Ro, S. T., 2003, "An Improved Analytic Model to Predict Fouling Phenomena in the Axial Flow Compressor of Gas Turbine Engines," *Proceedings of the International Gas Turbine Congress, Tokyo, Nov. 2–7, IGTC2003 Paper No. TS-095*, Tokyo.

[12] Seddigh, F., and Saravanamuttoo, H. I. H., 1991, "A Proposed Method for Assessing the Susceptibility of Axial Compressors to Fouling," J Eng Gas Turb Power, **113**(4), pp. 595–601.

[13] Diakunchak, I. S., 1992, "Performance Deterioration in Industrial Gas Turbines," J Eng Gas Turb Power, **114**(2), pp. 161–168.

[14] Greitzer, E. M., 1976, "Surge and Rotating Stall in Axial Flow Compressors Part 1: Theoretical Compresson System Model," J. Eng. Power, **98**, pp. 199–211.

[15] Hansen, K. E., Jørgensen, P., Larsen, P. S., Jorgensen, P., and Larsen, P. S., 1981, "Experimental and Theoretical Study of Surge in a Small Centrifugal Compressor," J. Fluids Eng., **103**(3), pp. 391–395.

[16] Greitzer, E. M., and Moore, F. K., 1986, "A Theory of Post-Stall Transients in Axial Compression Systems : Part I — Development of Equations," Trans. ASME, **108**(68).

[17] Fink, D. A., Cumpsty, N. A., and Greitzer, E. M., 1992, "Surge Dynamics in a Free Spool Centrifugal Compressor System," J. Turbomach., **114**, pp. 321–332.

[18] Gravdahl, J. T., and Egeland, O., 1997, "Speed and Surge Control for a Low Order Centrifugal Compressor Model," Proc. 1997 IEEE Int. Conf. Control Appl., pp. 344–349.

[19] Gravdahl, J. T., and Egeland, O., 1997, "A Moore-Greitzer Axial Compressor Model with Spool Dynamics," *Proceedings of the 36th Conference on Decision & Control, San Diego, California, USA. December, 1997*, IEEE.

[20] Macdougal, I., and Elder, R. L., 1983, "Simulation of Centrifugal Compressor Transient Performance for Process Plant Applications," J. Eng. Power, **105**(4), pp. 885–890.

[21] Spakovszky, Z. S., 2000, "Applications of Axial and Radial Compressor Dynamic System Modeling," Massachusetts Institute of Technology.

[22] PBS, 2016, "TJ100 Turbojet Engine" [Online]. Available: http://www.pbsvb.com/getattachment/Zakaznicka-odvetvi/Letectvi/Aircraft-

UAV-engines/Proudovy-motor-TJ-100/Turbojet-engine_TJ100.pdf.aspx. [Accessed: 14-Dec-2016].

[23] Jiri Pecinka, Adolf Jilek, Petr Kmoch, 2017, "Small Jet Engine Centrifugal Compressor Stability Margin Assessment," *Proceedings of ASME Turbo Expo 2017*, ASME.

[24] Yoon, S. Y., Lin, Z., and Allaire, P. E., 2013, "Control of Surge in Centrifugal Compressors by Active Magnetic Bearings," *Advances in Industrial Control*, Springer-Verlag, London, pp. 1–275.

[25] Aretakis, N., Mathioudakis, K., Kefalakis, M., and Papailiou, K., 2004, "Turbocharger Unstable Operation Diagnosis Using Vibroacoustic Measurements," J. Eng. Gas Turbines Power, **126**(4), pp. 840–847.

Figure Captions List

Table Caption List

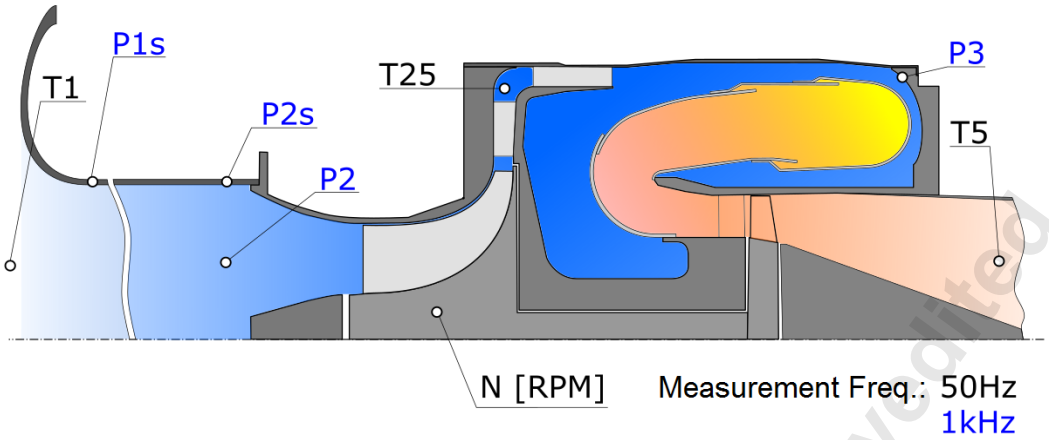

Fig. 1 Layout of small jet engine test rig showing measurement points

Fig. 2 Simulated fouling pattern in test rig compressor

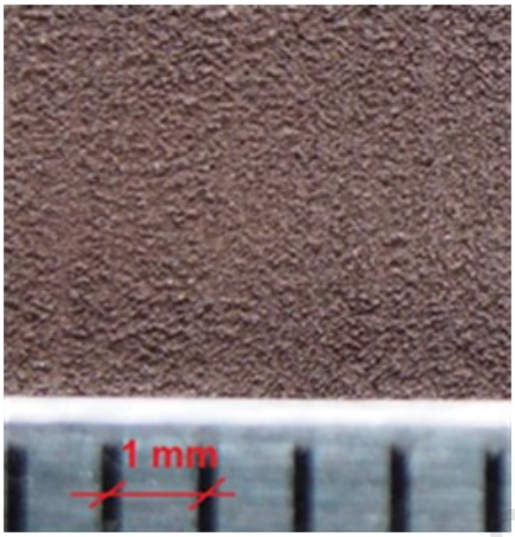

Fig. 3 Texturized fouling paint layer

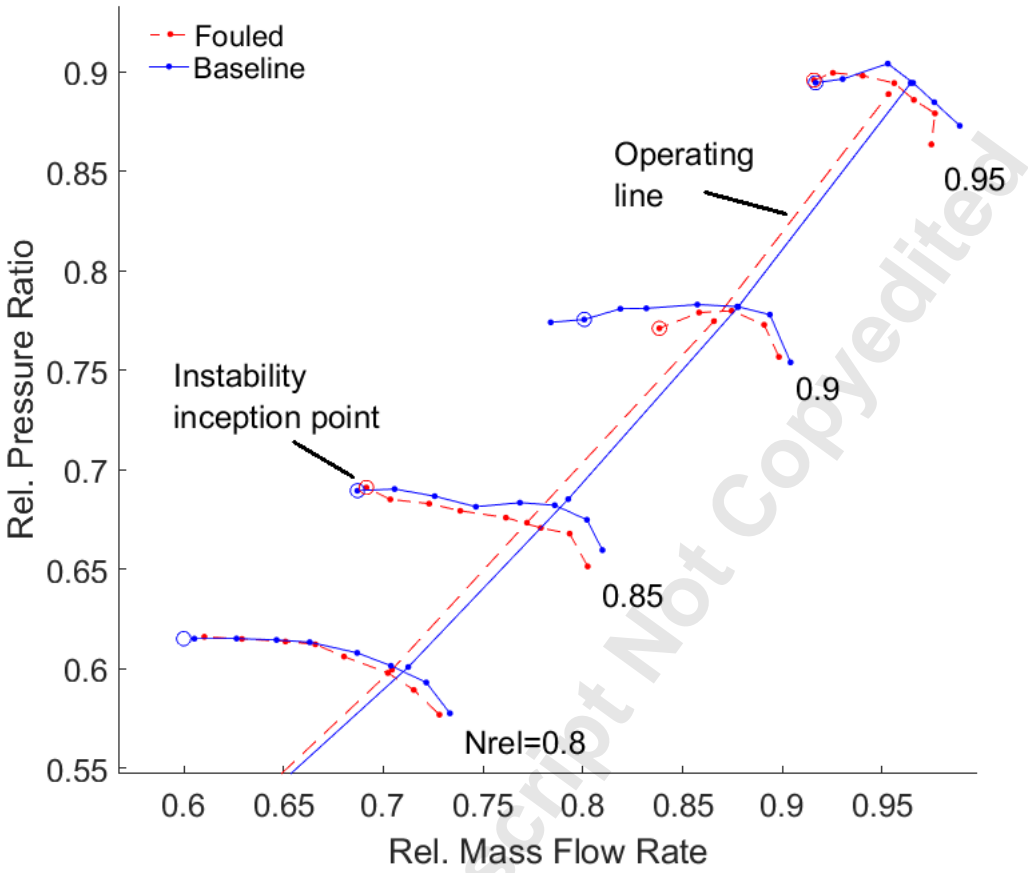

Fig. 4 Baseline vs fouled compressor pressure map

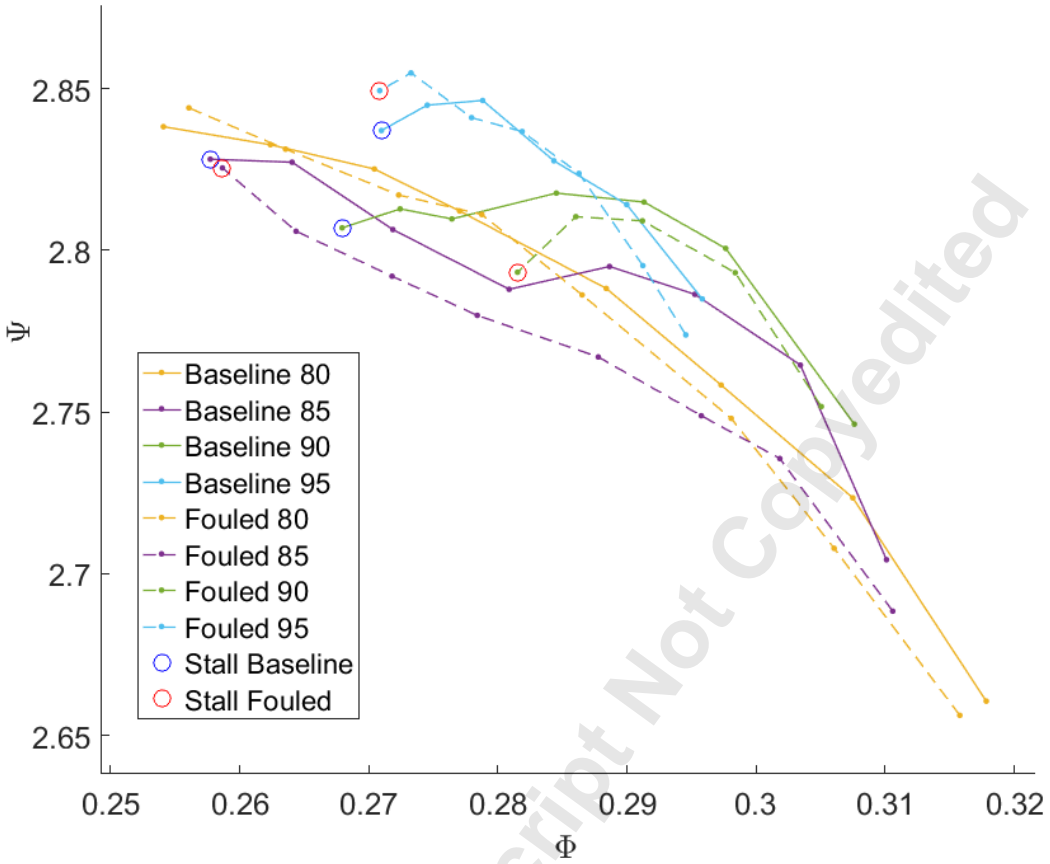

Fig. 5 Non-dimensional map of clean and fouled compressor

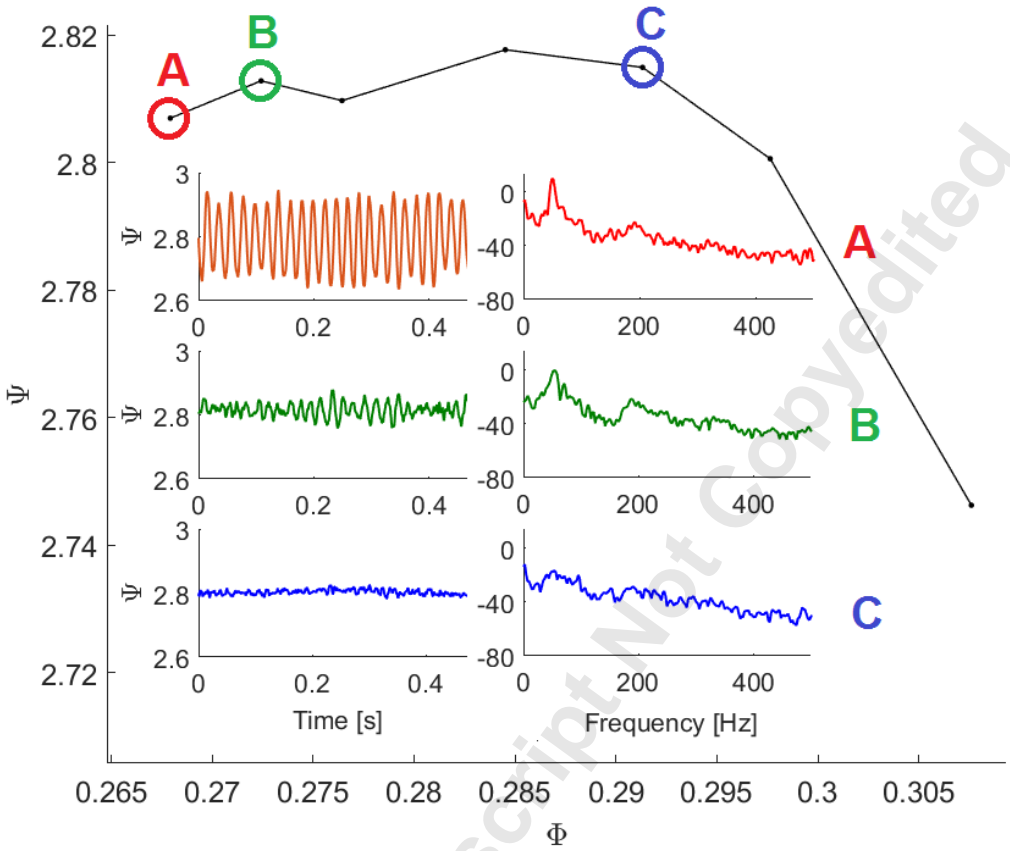

Fig. 6 Compressor discharge pressure oscillations in time and frequency domain for 90% RPM

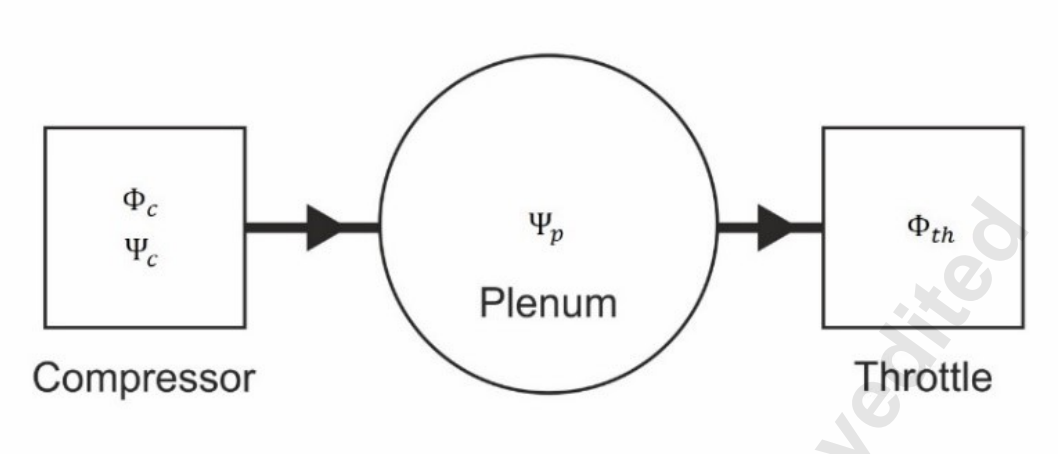

Fig. 7 Overview of a Greitzer compression system model

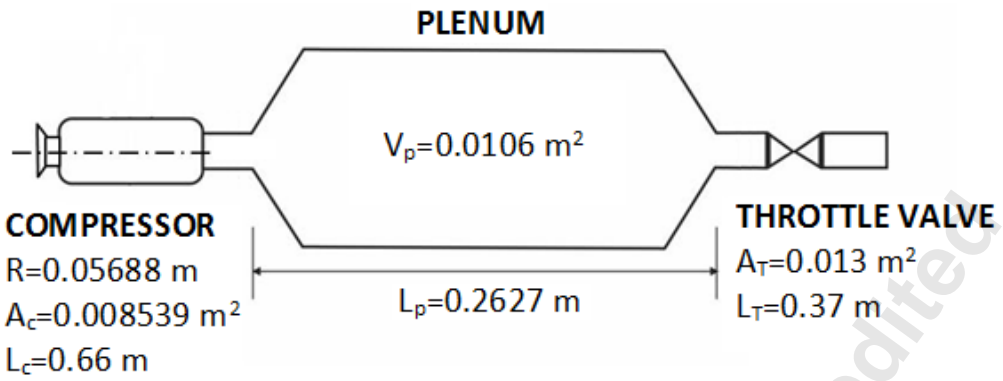

Fig. 8 Geometric parameter of experimental test

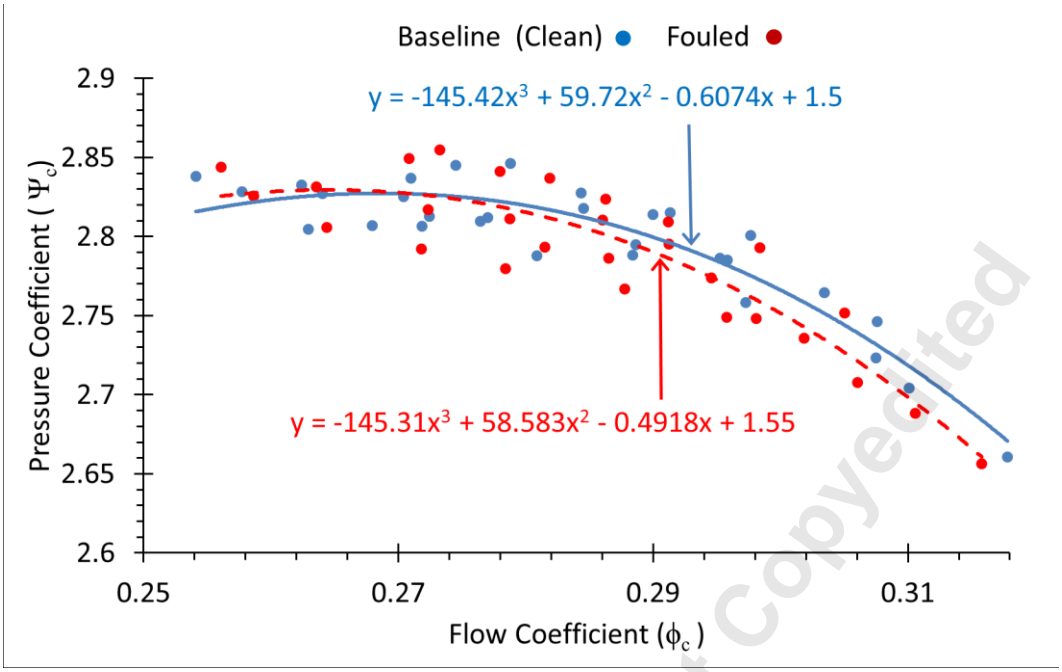

Fig. 9 Generalized pressure-rise characteristic for test rig based on experimental data

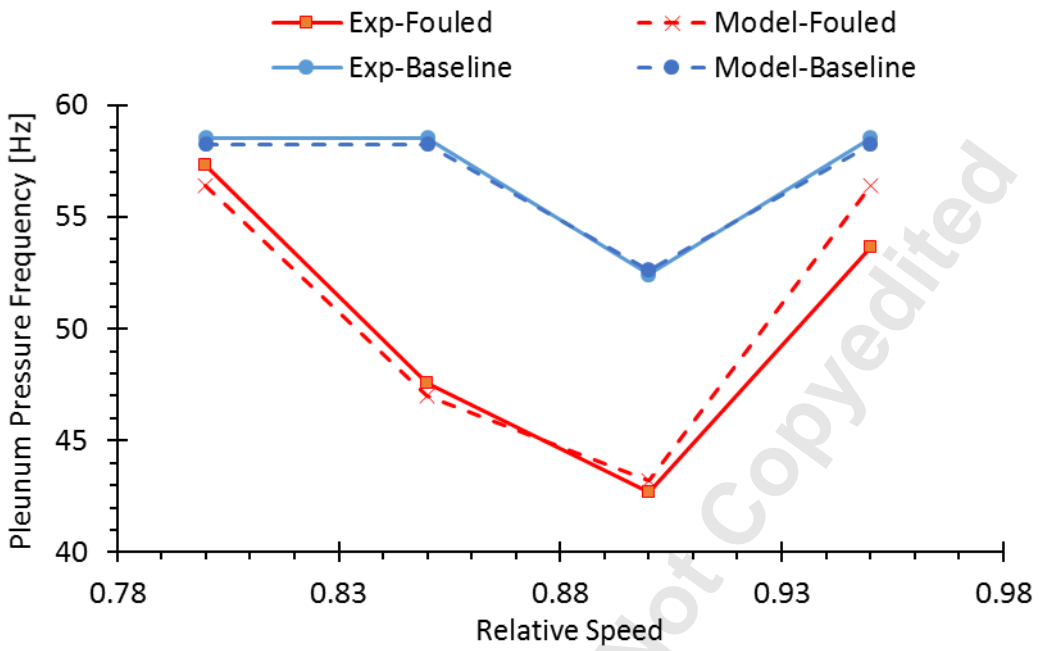

Fig. 10 Plenum pressure disturbance frequency for baseline and fouled operations

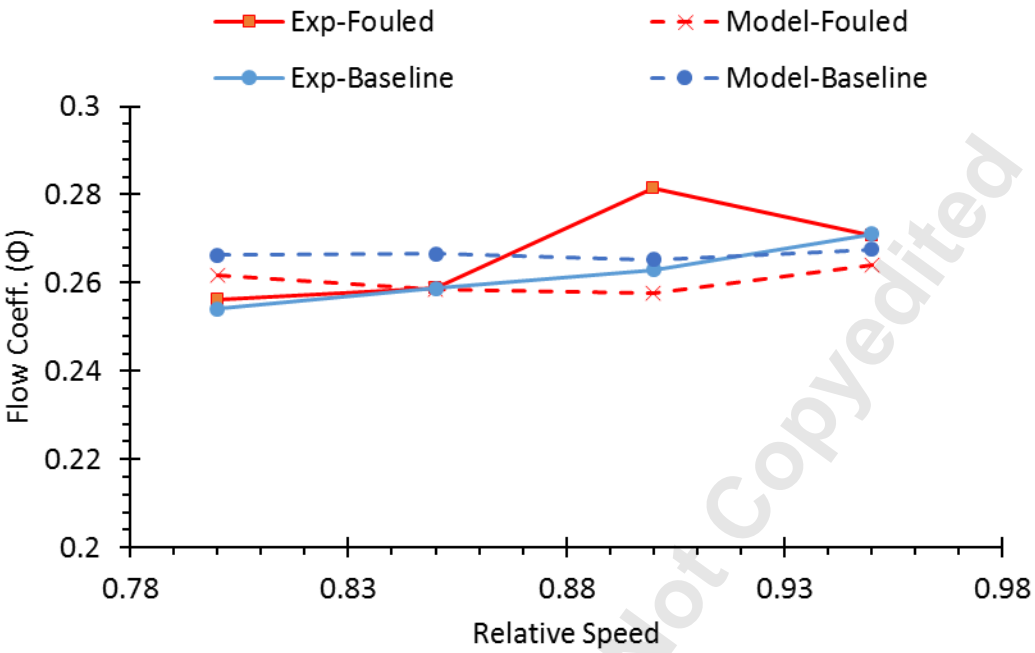

Fig. 11 Disturbance mean flow coefficient for baseline and fouled operations

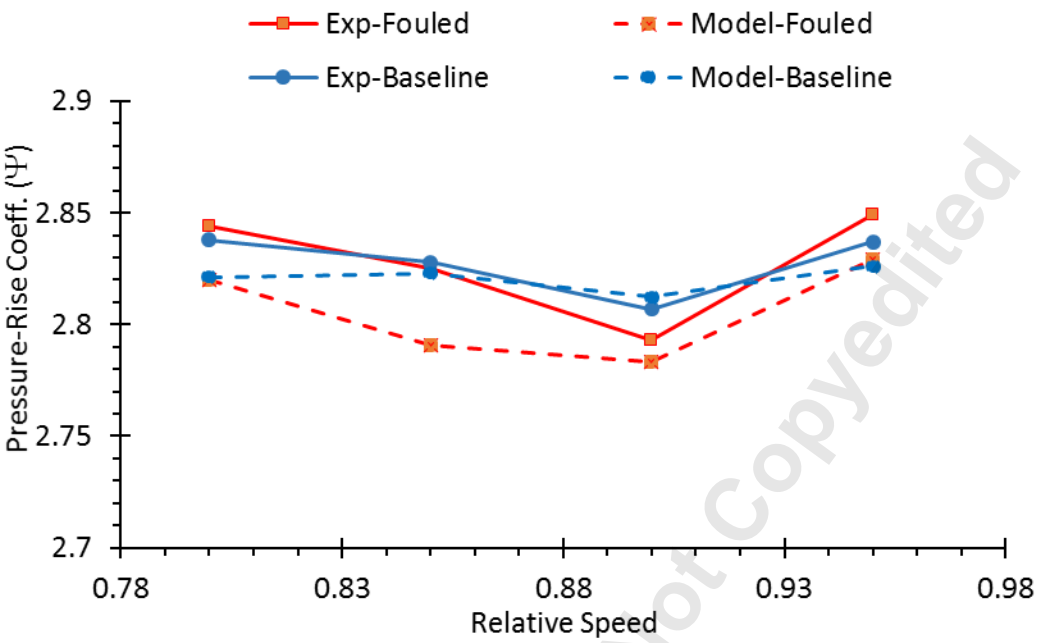

Fig. 12 Disturbance mean pressure-rise coefficient for baseline and fouled operations

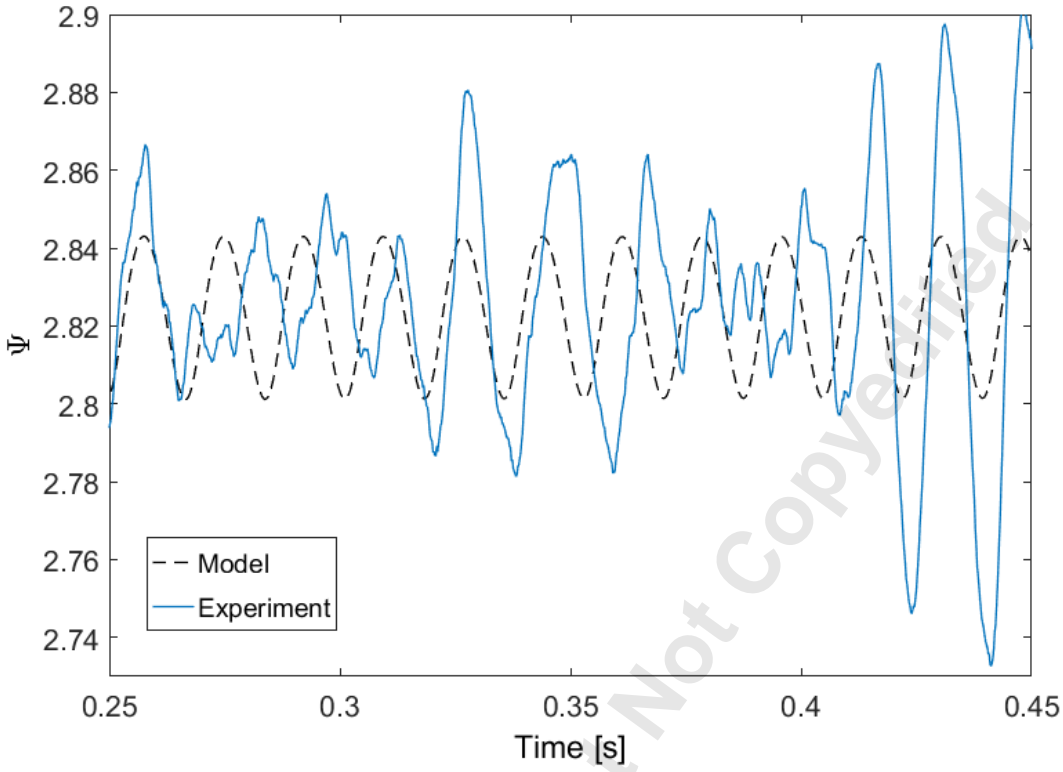

Fig. 13 Measured time waveform for the plenum pressure-rise coefficient at 0.85 of rated speed

Table 1 Throttle parameter at inception of instability

Speed [%]	80	85	90	95
S - Baseline	39.8	39.7	40	39.5
S - Fouled	41.2	41.9	41.8	40.6